



Synthesis of TiO₂ nanofibers by electrospinning using water-soluble Ti-precursor

Odhiambo Vincent Otieno¹ · Edina Csáki¹ · Orsolya Kéri¹ · László Simon² · István Endre Lukács³ · Katalin Mészáros Szécsényi⁴ · Imre Miklós Szilágyi¹

Received: 4 May 2019 / Accepted: 18 May 2019 / Published online: 29 May 2019
© The Author(s) 2019

Abstract

A new electrospinning process was developed for preparing TiO₂ nanofibers using a water-soluble Ti-precursor, [bis(kappa1O-hydroxo)(bis(kappa2O,O'-lactato)titanium(IV))] commonly known as titanium(IV) bis (ammonium lactato) dihydroxide (TiBALDH). The importance of the study is justified by the fact that Ti-precursors used for electrospinning, sol-gel, hydrothermal and other fiber synthesis processes are mostly non-water soluble. Accordingly, anatase TiO₂ nanofibers of diameter between 20 and 140 nm were synthesized by electrospinning and annealing. Polyvinylpyrrolidone (PVP) and different concentrations of TiBALDH were dissolved in a mixture of water, ethyl alcohol and acetic acid to optimize the electrospinning conditions. The thermal decomposition and fragmentation of PVP, TiBALDH and the fibers with 50% mass fraction of TiBALDH were studied by TGA-MS measurements. The fibers were then annealed at 1 °C min⁻¹ until 600 °C. The TiO₂ fibers were characterized using SEM-EDX, FTIR and XRD

Keywords TiBALDH · PVP · Electrospinning · Annealing · TiO₂ · TGA-MS · SEM-EDX · FTIR and XRD

Introduction

Titanium dioxide is used in a number of applications including self-cleaning, antimicrobial thin film coatings, photocatalysis, gas sensing and dye-sensitized solar cells [1–5]. This has led to a lot of research in the preparation of

TiO₂ nanofibers with well-controlled morphology [6–10]. Many methods of synthesis of TiO₂ nanofibers have been developed including sol-gel, hydrothermal and electrospinning [11–13]. Electrospinning as a method of synthesis of nanofibers has been widely reported [14–17]. The technique is a versatile and efficient method for synthesizing uniform fibers with large specific surface area [18–21]. In electrospinning, high static voltage is applied to a polymer solution or melt, which can contain a precursor salt of metal oxide in a syringe. The solution or melt is ejected from the needle tip, accelerated by electric field and is collected on a grounded substrate in form of thin continuous fibers [17, 22–24]. The nanofiber properties can be controlled to offer more flexibility in surface functionalities of the end product. Many studies use Ti-alkoxides and Ti-halides as precursors for the synthesis of TiO₂; however, these are insoluble in water [25]. There is a need to prepare TiO₂ nanofibers from water-soluble precursors. This would enable coupling TiO₂ with other metal oxides having water-soluble precursors. In this study, [bis(kappa1O-hydroxo)(bis(kappa2O,O'-lactato)titanium(IV))] commonly known as titanium(IV) bis (ammonium lactato) dihydroxide (TiBALDH) was used as the precursor in preparing

Electronic supplementary material The online version of this article (<https://doi.org/10.1007/s10973-019-08398-z>) contains supplementary material, which is available to authorized users.

✉ Odhiambo Vincent Otieno
vincent.odhiambo@mail.bme.hu

¹ Department of Inorganic and Analytical Chemistry, Budapest University of Technology and Economics, Szent Gellért tér 4., Budapest 1111, Hungary

² Department of Organic Chemistry and Technology, Budapest University of Technology and Economics, Budafoki út 8., Budapest 1111, Hungary

³ Research Institute for Technical Physics and Materials Science, Hungarian Academy of Sciences, Konkoly Thege M. út 29-33., Budapest 1121, Hungary

⁴ Department of Chemistry, Biochemistry and Environmental Protection, University of Novi Sad, Trg Dositeja Obradovica 3, 21000 Novi Sad, Serbia

TiO₂ nanofibers. The structure of TiBALDH is shown in Fig. 1.

TiBALDH is a water-soluble titanium precursor with low reactivity [26, 27]. It has been used to make various titania nanomaterials. Mockel et al. reported that TiBALDH was utilized to produce almost monodispersed anatase nanocrystals by thermohydrolysis [28]. Mayya et al. [29] reported a nanoscale coating of gold nanoparticles with titania based on TiBALDH. Lee et al. [30] prepared anatase TiO₂ nanoparticles coupled with carbon nanotubes (CNTs) by controlled hydrolysis of TiBALDH in CNTs containing aqueous media. Hongzhi et al. [31] prepared TiO₂ nanocrystals by hydrolysis and hydrothermal treatment of TiBALDH. There is only one report in which a water-soluble TiO₂ precursor was used to synthesize TiO₂ nanofibers by electrospinning. Nakane et al. [32] prepared hybrid nanofibers of poly(vinyl-alcohol) and titanium lactate by electrospinning. In their study, Nakale et al did not optimize the

concentration for the precursors and only one set of concentration was published. However, no studies have been reported about the use of TiBALDH as a precursor in the synthesis of TiO₂ nanofibers by electrospinning. There are also no reports on thermal analysis of TiBALDH which is important since to obtain crystalline TiO₂, an annealing step is often needed.

In this study, TiO₂ nanofibers were prepared by electrospinning a mixture of alcoholic and aqueous solutions of polyvinylpyrrolidone (PVP) and TiBALDH. We studied how the properties of the electrospun fibers could be controlled by using different concentrations of the precursor. The thermal decomposition and fragmentation of PVP, TiBALDH and the fiber with 50% mass fraction of TiBALDH were studied by TGA-MS measurements. The thermal properties of the electrospun fibers were investigated in nitrogen by simultaneous thermogravimetry/differential thermal analysis (TG/DTA). The electrospun fibers were annealed at 600 °C to remove the polymer component, decompose the precursor and obtain TiO₂ nanofibers. The electrospun and annealed nanofibers were characterized by scanning electron microscopy (SEM) and energy-dispersive X-ray spectroscopy (EDX). The fibers, PVP and TiBALDH were studied by Fourier transform infrared spectroscopy (FTIR). The annealed fibers were investigated by X-ray diffraction (XRD).

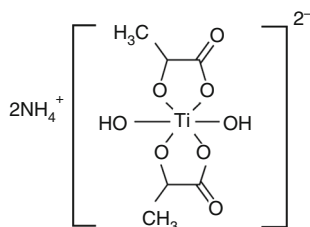


Fig. 1 Structure of TiBALDH

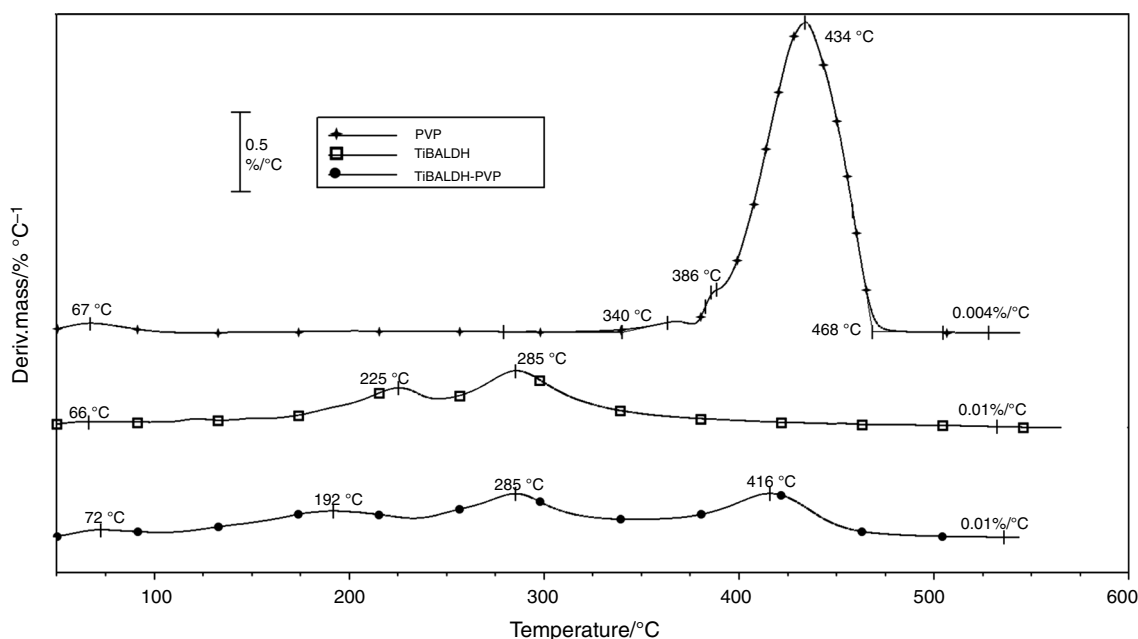


Fig. 2 DTG curves of PVP, TiBALDH and PVP-TiBALDH mixture in argon

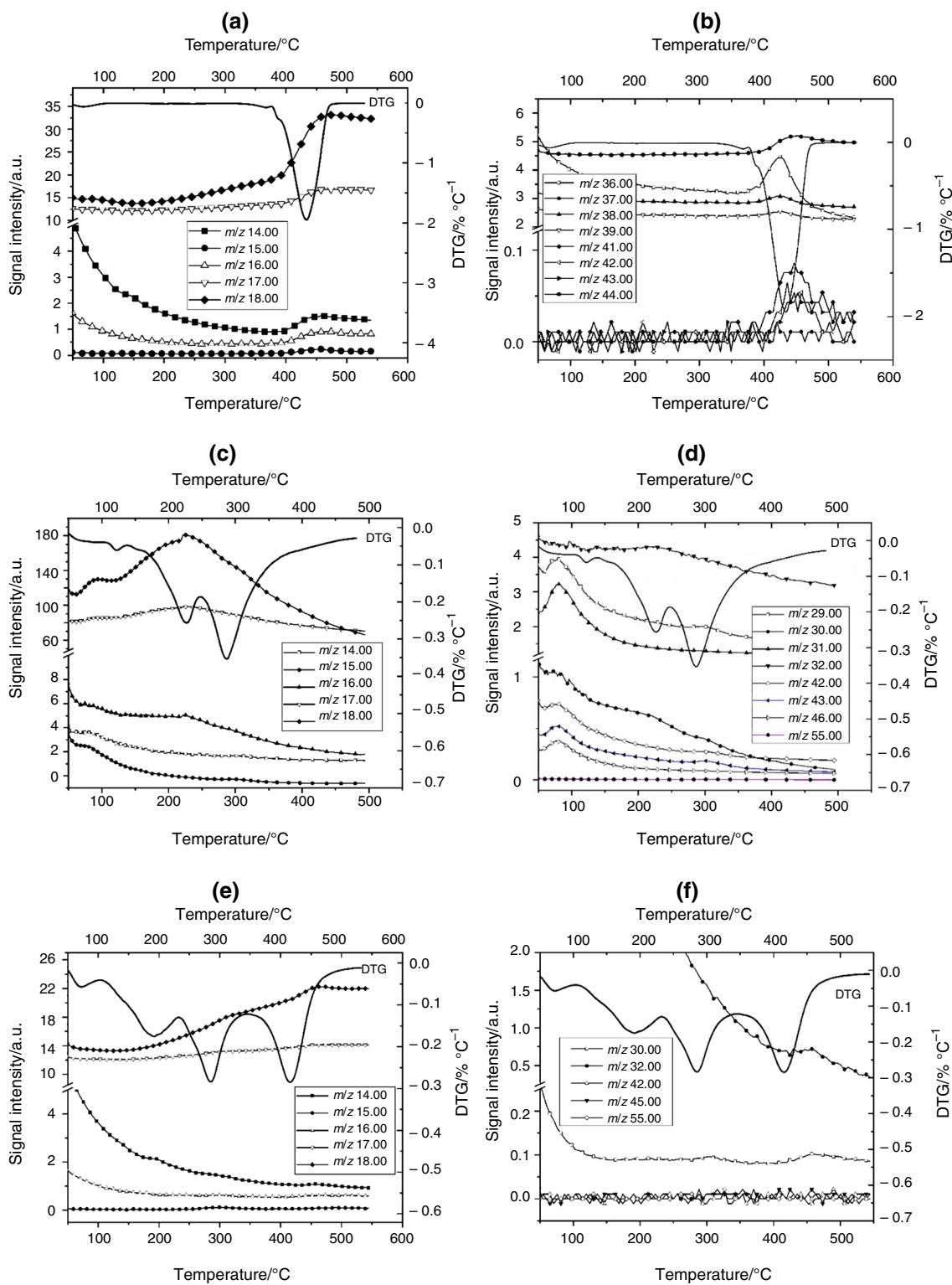


Fig. 3 DTG-MS curves of PVP (a, b) TiBALDH (c, d) and PVP-TiBALDH mixture (e, f) in argon

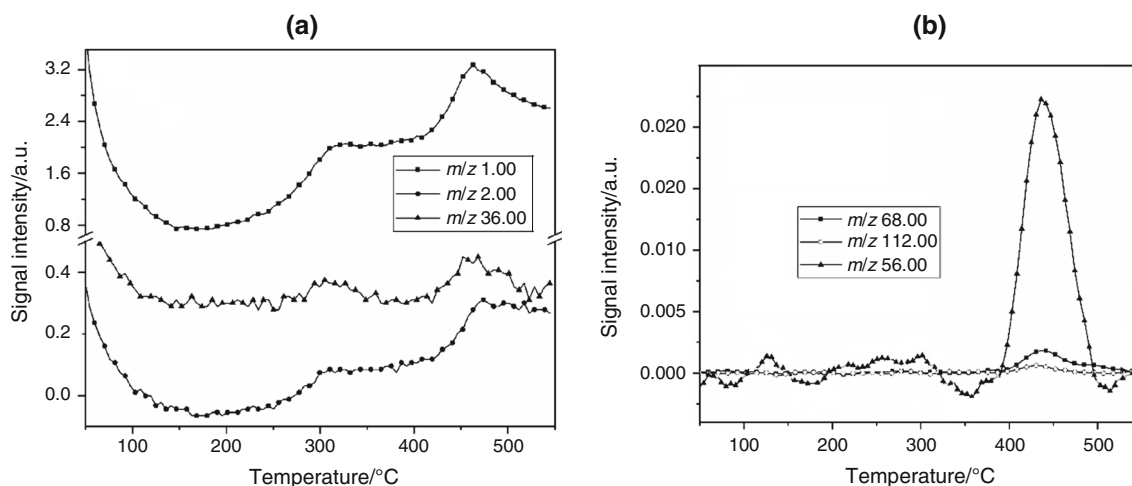


Fig. 4 MS curve for other characteristic fragments of PVP decomposition in argon

Experimental

Materials

All materials were analytical grade and used as received. Polyvinylpyrrolidone [PVP, $(C_6H_9NO)_n$, K-90] and titanium(IV) bis(ammonium lactato)dihydroxide [$(C_6H_{18}N_2O_8Ti)$ TiBALDH, 50 mass% in water] were obtained from Sigma-Aldrich.

Preparation and characterization of TiO_2 fibers

The polymer solution contained 20 mass% PVP dissolved in 1:1 mixture of acetic acid and ethyl alcohol. 2 mL of the polymer solution was mixed with 2 mL of an aqueous solution containing 50, 30, 25 and 10 mass% TiBALDH, respectively. The mixture was stirred for 6 h at room temperature. The mixed solution was loaded into a plastic syringe equipped with a needle for electrospinning. The feeding rate was 1 mL h^{-1} , while the applied voltage was 25 kV. The fibers were collected on an Al foil screen covered by a polyethylene sheet.

For the thermal measurements, a 50 mass% solution of TiBALDH was carefully¹ dried. TG/DTA–MS measurements for TiBALDH, PVP and as-spun fiber of 50 mass% TiBALDH were carried out using the TA Instruments' Q600 simultaneous TG/DSC setup coupled to a Hiden Analytical HPR-20/QIC mass spectrometer. The measurements were carried out in flowing argon (flow rate = $50 \text{ cm}^3 \text{ min}^{-1}$) in an alumina crucible and empty crucible as a reference. The sample mass was ca. 7 mg. Selected ions between $m/z = 1\text{--}125$ were monitored in

multiple ion detection mode (MID) at a heating rate of $10 \text{ }^\circ\text{C min}^{-1}$.

The electrospun fibers were annealed in air to remove the polymer and decompose the precursor. The annealing was done at a rate of $1 \text{ }^\circ\text{C min}^{-1}$ up to $600 \text{ }^\circ\text{C}$. The thermal decomposition of the electrospun fibers in nitrogen was investigated in an STD 2960 simultaneous DTA/TGA (TA Instruments Inc.) thermal analyzer. The samples were heated up to $600 \text{ }^\circ\text{C}$ using a heating rate of $10 \text{ }^\circ\text{C min}^{-1}$ in nitrogen.

The morphology of the as-spun fibers was studied by scanning electron microscopy (SEM) in a JEOL JSM-5500LV scanning electron microscope in a high vacuum mode at 20 kV. For the annealed samples, the SEM images were observed by a LEO 1440 XB electron microscope in a high vacuum mode with secondary electron detector. The EDX analysis of the annealed fibers was done using JEOL JSM-5500LV electron microscope. Before the measurement, the nanofibers were coated with a thin Au/Pd layer in a sputter coater. Fourier transform infrared spectroscopy (FTIR) measurements of carefully dried 50 mass% TiBALDH, PVP, electrospun and annealed nanofibers were recorded with a Nicolet 6700 apparatus in the $400\text{--}4000 \text{ cm}^{-1}$ domain in transmittance mode. The sensitivity of measurements was 4 cm^{-1} , and 64 scans were accumulated per spectrum. The XRD patterns were recorded by a PANalytical X'pert Pro MPD X-ray diffractometer using $Cu K_\alpha$ irradiation.

Results and discussion

TG/DTA–MS measurements were carried out to study how the TiO_2 precursor, TiBALDH, affects the decomposition of PVP and the formation of TiO_2 . Figure 2 shows that the

¹ According to the Safety Information the hazard statement of TiBALDH is H226-H319.

decomposition of TiBALDH is continuous showing two DTG maxima to 550 °C, while the decomposition of PVP takes place in practically one step between 340 and 468 °C without residue [33, 34]. The decomposition of the fiber with 50 mass% TiBALDH and 20% PVP is also continuous with three DTG maxima up to 550 °C. The decomposition

of the fiber and both of its components is practically finished around 550 °C. In the temperature range up to about 100 °C, the evaporation of the solvents is expected.

The DTG–MS data are shown in Fig. 3a–f. In the samples of PVP (Fig. 3a) and the fiber of PVP/50 mass% TiBALDH (Fig. 3e), at first, water evaporation was

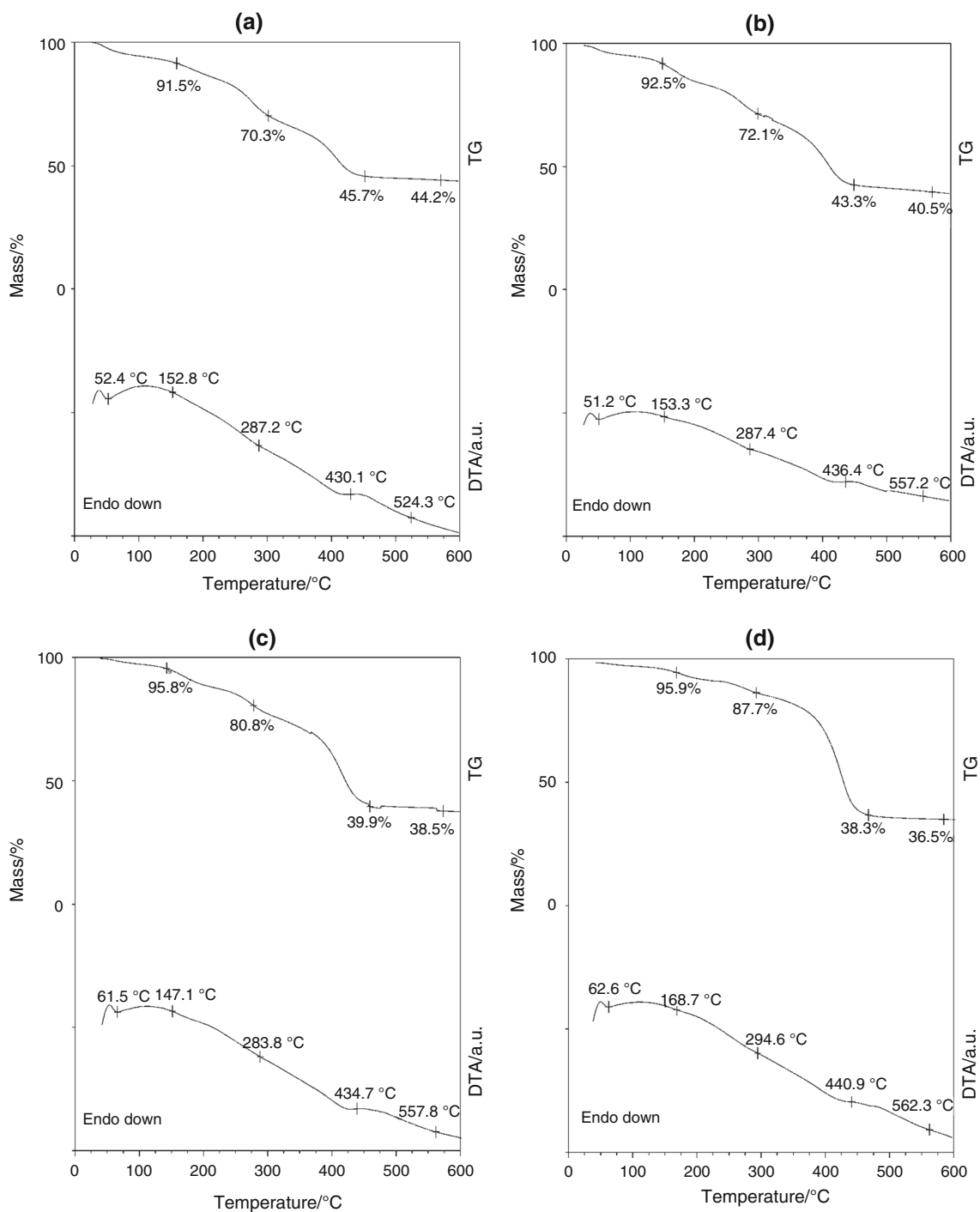


Fig. 5 TG/DTA of as-spun fibers in nitrogen **a** 50 mass% TiBALDH, **b** 30 mass% TiBALDH, **c** 25 mass% TiBALDH and **d** 10 mass% TiBALDH

detected. In addition, in TiBALDH, the appearance of fragments with 14–18 and 29–46 m/z ratio indicates a partial decomposition of the TiO_2 precursor even below 100 °C (Fig. 3c, d). This is not surprising taking into account the hazard statements of TiBALDH. Above 100 °C, in the DTG curve of the composite fiber, the peaks characteristic for both of PVP and of TiBALDH was observed. However, the DTG maxima appeared at lower temperatures than in the pure components.

The most intense MS signals of PVP are those with $m/z = 18$ and 17. The intensity ratio of the peaks below 100 °C agrees with that of water. At higher temperatures, the intensity ratio changes as a result of the evolution of fragments NH_3^+ and NH_4^+ . The intensity of the signals of

the fragments with $m/z = 14, 15$ and 16 is about ten times less than of fragments $m/z = 18$ and 17. Besides these, low-intensity signals with a higher m/z ratio were also detected (Fig. 3b). The courses of the m/z signals follow well the course of the DTG signal. Since the decomposition was recorded in flowing argon using TG/DTA-MS, relative intense signals of H^+ and H_2^+ ($m/z = 1, 2$) and C_3^+ ($m/z = 36$) were detected due to the reduction of the polymer (Fig. 4a). The molecular fragment of the PVP monomer with $m/z = 111$ was not found. The fragment with the highest m/z was detected at 112 (Fig. 4b) which most probably originates from the recombination of the fragment with $m/z = 56$ (see Fig. 4b). Besides, a low-intensity signal in PVP was detected at $m/z = 68$. The appearance of these

Table 1 As-spun and annealed fiber diameters and composition of annealed fibers

| TiBALDH/mass% | As-spun fibers d/nm | Annealed fibers d/nm | Atomic/% | |
|---------------|------------------------------|-------------------------------|----------|------|
| | | | Ti | O |
| 50 | 617–800 | 131–168 | 35.8 | 64.2 |
| 30 | 487–608 | 61–82 | 38.9 | 61.1 |
| 25 | 425–453 | 41–68 | 35.5 | 64.5 |
| 10 | 309–375 | 20–57 | 34.5 | 65.5 |

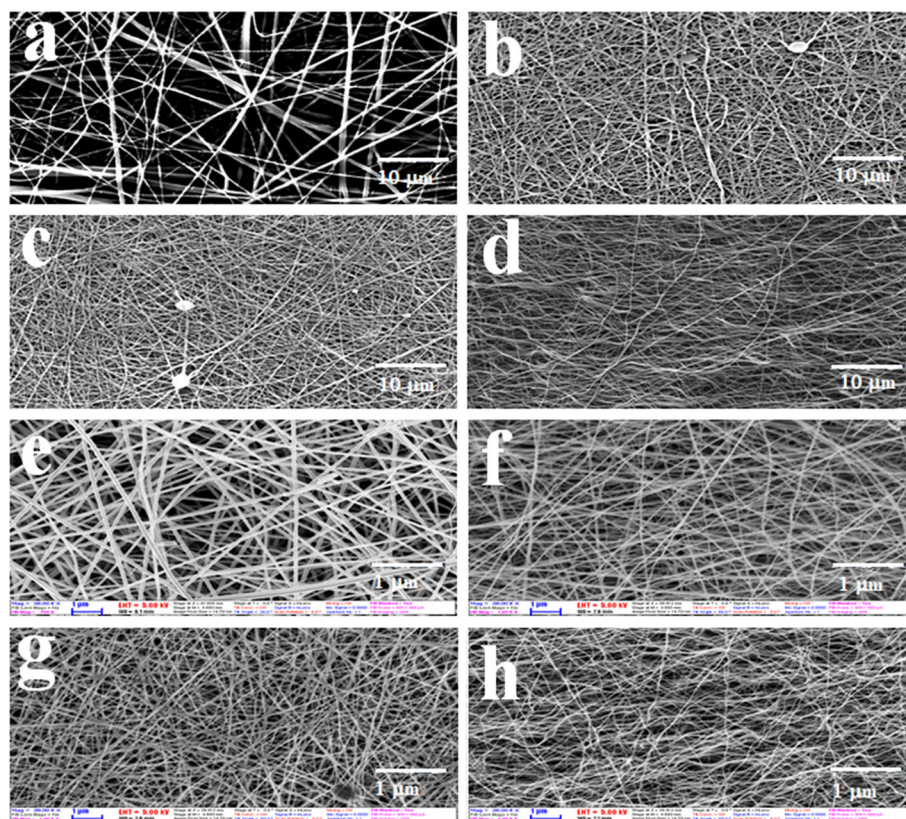


Fig. 6 SEM images of **a** as-spun fibers 50 mass% TiBALDH, **b** as-spun fibers 30 mass% TiBALDH, **c** as-spun fibers 25 mass% TiBALDH, **d** as-spun fibers 10 mass% TiBALDH, **e** annealed fibers

50 mass% TiBALDH, **f** annealed fibers 30 mass% TiBALDH, **g** annealed fibers 25 mass% TiBALDH, **h** annealed fibers 10 mass% TiBALDH

signals is most probably a result of the fragmentation of the pyrrolidone ring (*e.g.*, C₂H₂NO and C₃H₂NO).

During the decomposition of TiBALDH, only signals up to $m/z = 46$ ratio were detected (Fig. 3c, d). Fragments with $m/z = 18$, 29 and 31 had the most intense signals. These could be attributed to H₂O⁺, C₂H₅⁺ and C₂H₂OH⁺ formed during the decomposition of TiBALDH (C₆H₁₈N₂O₈Ti).

The difference in the fragmentation of the as-spun fiber compared to the fragmentation of the components used for its preparation is that in the mixture all the detected signals were below $m/z = 32$ (Fig. 3f). This means that in the preparation of the TiO₂ fibers TiBALDH catalyzes the decomposition of PVP.

Due to the very small differences in the molar masses of the expected CO₂⁺, N₂O⁺, NO_x⁺ fragments, their identification by this way was not possible. Based on the TGA measurements, the as-spun fibers should be annealed to 600 °C to obtain TiO₂ fibers.

Figure 5 shows the comparison of various composite fibers in nitrogen and that the decomposition is continuous. The endothermic peaks in the DTA peaks are not sharp, because the precursor and the polymer components of the fibers decomposed without combustion. The decomposition occurred in three stages as discussed earlier. The mass of the residues was consistent with the increasing concentration of the precursor. The percentage yield for the TiO₂ fibers varied depending on the concentration of the precursor, 50 mass% TiBALDH was 13.1%, 30 mass%

TiBALDH was 10.7%, 25 mass% TiBALDH was 10.4% and 10 mass% TiBALDH was 9.4%.

The as-spun PVP/TiBALDH fibers had diameters between 310 and 800 nm depending on the concentration of TiBALDH. The fibers were annealed in air at a heating rate of 1 °C min⁻¹ up to 600 °C. The slow heating rate was used to avoid disintegration of the oxide fibers [22]. The diameter of the as-spun and annealed fibers was larger when the concentration of TiBALDH was higher. After annealing, diameter of the fibers decreased significantly after annealing to 20–170 nm, as shown in Table 1.

From the SEM image of annealed fibers shown in Fig. 6, the fibers formed from 50 mass% and 30 mass% TiBALDH were smooth, while the fibers from 25 mass% and 10 mass% TiBALDH had some beads.

Results of EDX analysis are shown in Fig. 7. They confirmed the presence of titanium and oxygen in the annealed fibers. Ti peak was observed at 4.5 kV [35, 36]. The elemental composition in the annealed fibers is as shown in Table 1.

The results for the FTIR measurements of pure TiBALDH, PVP, as-spun and annealed composite fibers are shown in Fig. 8. The broadband around 3600 cm⁻¹ can be assigned to O–H stretching vibration while the peak around and 3200 cm⁻¹ can be due to N–H stretching vibrations in TiBALDH. The C–H asymmetric vibrations of the methyl group in TiBALDH and PVP were observed around 2980 cm⁻¹. The sharp absorption bands around 1639 cm⁻¹ can be assigned to C=O in the amide group in

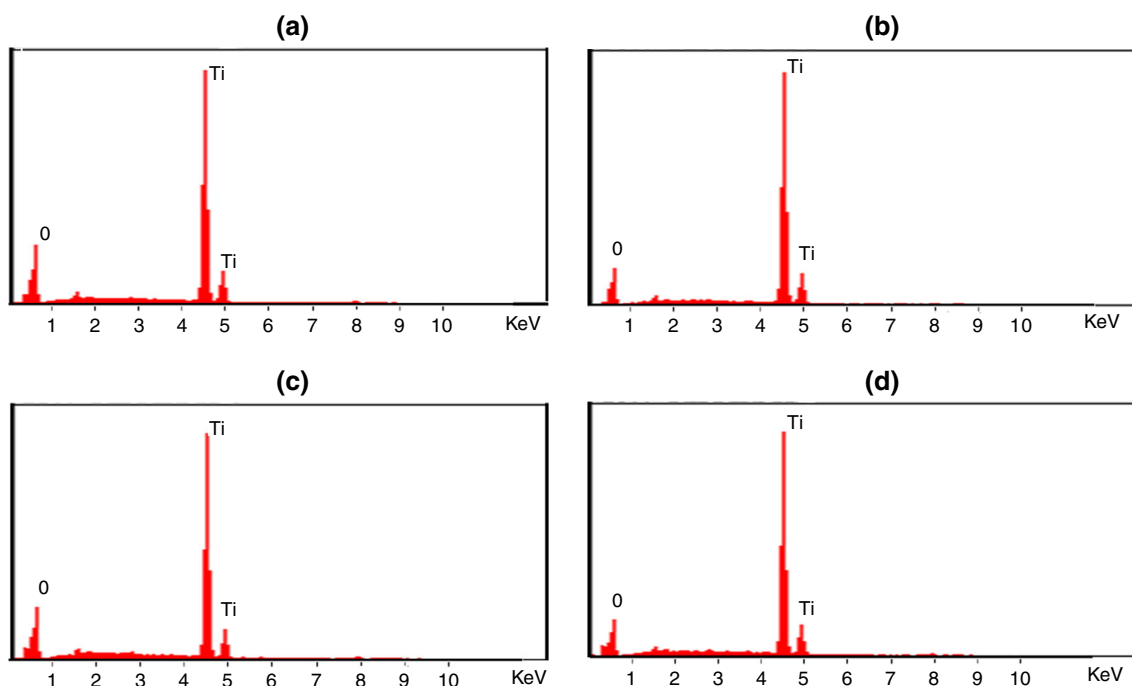


Fig. 7 EDX spectra of annealed fibers **a** 50 mass% TiBALDH, **b** 30 mass% TiBALDH, **c** 25 mass% TiBALDH and **d** 10 mass% TiBALDH

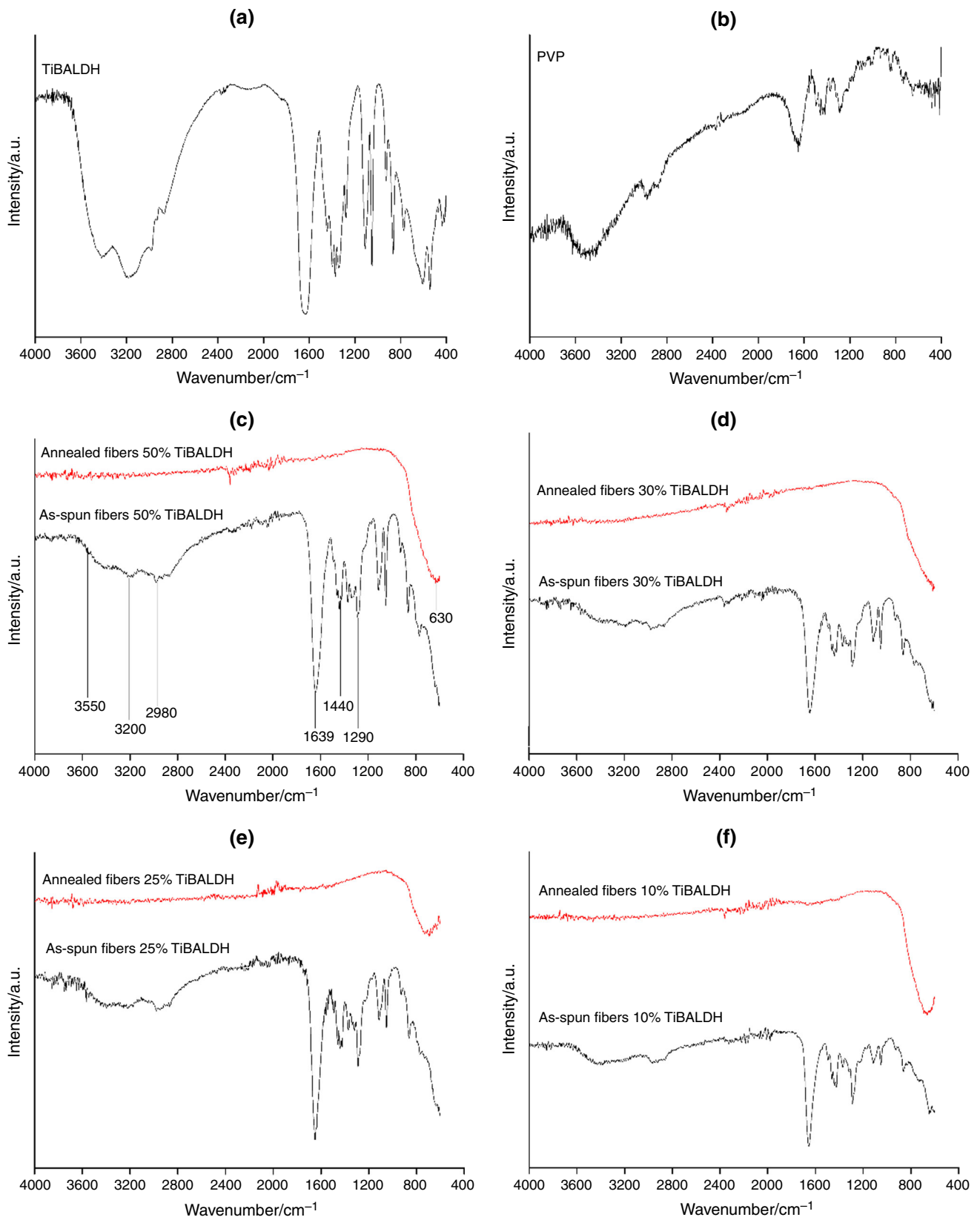


Fig. 8 FTIR spectra of as-spun and annealed fibers **a** TiBALDH, **b** PVP, **c** 50 mass% TiBALDH, **d** 30 mass% TiBALDH, **e** 25 mass% TiBALDH and **f** 10 mass% TiBALDH

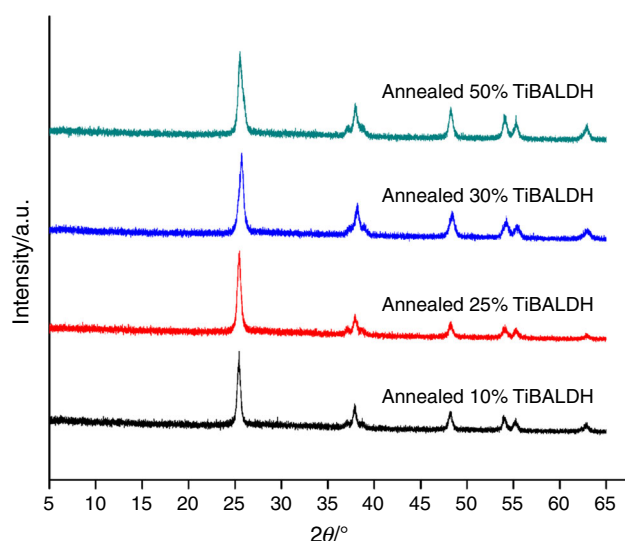


Fig. 9 XRD patterns of annealed fibers

PVP. The peak around 1440 cm^{-1} can be assigned to O–H bending vibrations. The C–N stretching vibration absorption peaks in PVP were observed around 1290 cm^{-1} [33, 37, 38]. These absorption bands were also observed in the as-spun fibers. For the annealed samples, the absorption band around 630 cm^{-1} can be assigned to the Ti–O–Ti bonds [37]. The FTIR measurements of the annealed fibers confirmed that the polymer and the precursor were decomposed during annealing.

Figure 9 shows the XRD pattern of the annealed fibers. The fibers were crystalline with tetragonal structures. The XRD patterns exhibited strong diffraction peaks at 25° and 48° indicating TiO₂ in anatase phase [35, 39]. The annealed fibers were indexed to ICDD 04-016-2837.

Conclusions

Anatase TiO₂ nanofibers of diameter between 20–170 nm were synthesized by electrospinning using a water-soluble Ti-precursor. Polyvinylpyrrolidone and different concentrations of TiBALDH were dissolved in a mixture of water, ethyl alcohol and acetic acid followed by electrospinning at 20 kV to obtain nanofibers. The as-spun fibers were studied by TG/DTA-MS to establish annealing temperatures. The data of TGA-MS measurements revealed that TiBALDH catalyzes the decomposition of the as-spun fibers. During its decomposition, only fragments with $m/z < 32$ evolved. The fibers were annealed at $1\text{ }^\circ\text{C min}^{-1}$ until $600\text{ }^\circ\text{C}$ to form anatase TiO₂ nanofibers. 50 mass% and 30 mass% TiBALDH concentrations formed smooth fibers.

Acknowledgements Open access funding provided by Budapest University of Technology and Economics (BME). I. M. Szilágyi

thanks for a János Bolyai Research Fellowship of the Hungarian Academy of Sciences and an ÚNKP-18-4-BME-238 New National Excellence Program of the Ministry of Human Capacities, Hungary. A GINOP-2.2.1-15-2017-00084, an NRDI K 124212 and an NRDI TNN_16 123631 grants are acknowledged. The research within project No. VEKOP-2.3.2-16-2017-00013 was supported by the European Union and the State of Hungary, co-financed by the European Regional Development Fund. The research reported in this paper was supported by the Higher Education Excellence Program of the Ministry of Human Capacities in the frame of Nanotechnology and Materials Science research area of Budapest University of Technology (BME FIKP-NAT) and Stipendium Hungaricum scholarship grant. Katalin Mészáros Szécsényi thanks the Ministry of Education, Science and Technological Development, Serbia (Project Number: ON172014)

Open Access This article is distributed under the terms of the Creative Commons Attribution 4.0 International License (<http://creativecommons.org/licenses/by/4.0/>), which permits unrestricted use, distribution, and reproduction in any medium, provided you give appropriate credit to the original author(s) and the source, provide a link to the Creative Commons license, and indicate if changes were made.

References

- Liu S, Liu B, Nakata K, Ochiai T, Murakami T, Fujishima A. Electrospinning preparation and photocatalytic activity of porous TiO₂ nanofibers. *J Nanomater*. 2012;2012:1–5.
- Kéri O, Kócs L, Hörvölgyi Z, Baji Z, László K, Takáts V, et al. Photocatalytically active amorphous and crystalline TiO₂ prepared by atomic layer deposition. *Period Polytech Chem Eng*. 2019;63(3):378–87.
- Justh N, Mikula GJ, Bakos LP, Nagy B, László K, Párditka B, et al. Photocatalytic properties of TiO₂@polymer and TiO₂@carbon aerogel composites prepared by atomic layer deposition. *Carbon N Y*. 2019;147:476–82. <https://doi.org/10.1016/j.carbon.2019.02.076>.
- Sylwia W. Titanium dioxide doped with vanadium as effective catalyst for selective oxidation of diphenyl sulfide to diphenyl sulfonate. *J Therm Anal Calorim*. 2018;9:1471–80.
- Gonzalez-Calderon JA, Pérez-Pérez C, Pérez-Rodríguez RY, Fierro-González JC, Vallejo-Montesinos J. Silanization of di-n-octyldichlorosilane as a route to improve the integration of titanium dioxide in polypropylene. *J Therm Anal Calorim*. 2019;0123456789. <https://doi.org/10.1007/s10973-019-08159-y>.
- Albetran H, Dong Y, Low IM. Characterization and optimization of electrospun TiO₂ /PVP nanofibers using Taguchi design of experiment method. *J Asian Ceram Soc*. 2015;3:292–300.
- Kéri O, Bárdos P, Boyadzhiev S, Igricz T, Nagy ZK, Szilágyi IM. Thermal properties of electrospun polyvinylpyrrolidone/titanium tetraisopropoxide composite nanofibers. *J Therm Anal Calorim*. 2019. <https://doi.org/10.1007/s10973-019-08030-0>.
- Boyadzhiev S, Georgieva V, Rassovska M. QCM gas sensor characterization of ALD-grown very thin TiO₂ films QCM gas sensor characterization of ALD-grown very thin. *Journal of Physics Conference Series*. 2018.
- Choi HS, Kim T, Im JH, Park CR. Preparation and electrochemical performance of hyper-networked Li₄Ti₅O₁₂ / carbon hybrid nanofiber sheets for a battery–supercapacitor hybrid system. *Nanotechnology*. 2011;22:405402.
- Keshavarz M, Zebarjad SM, Daneshmanesh H, Moghim MH. On the role of TiO₂ nanoparticles on thermal behavior of flexible

- polyurethane foam sandwich panels. *J Therm Anal Calorim.* 2017;127:2037–48.
11. D. A. Matolygina, A. E. Baranchikov VKI. Synthesis of superfine titania via high temperature hydrolysis of titanium(IV) bis(ammonium lactato) dihydroxide. [cited 2018 Dec 9]; <https://link.springer.com/content/pdf/10.1134/S0012500811120019.pdf>.
 12. C. Tekmen, A. Suslu UC. Titania nanofibers prepared by electrospinning. [cited 2019 Jan 10]; http://hifyber.com/images/whitePapers/2008_Titania-nanofibers-prepared-by-electrospinning.pdf.
 13. Szilágyi IM, Nagy D. Review on one-dimensional nanostructures prepared by electrospinning and atomic layer deposition. In: *Journal Physics Conference Series.* 2014; vol 559.
 14. Obradovic N, Pavlovic V. Thermal, morphological, and mechanical properties of ethyl vanillin immobilized in polyvinyl alcohol by electrospinning process. *J Therm Anal Calorim.* 2014;118:661–8.
 15. Awal A, Sain M, Chowdhury M. Thermal analysis and spectroscopic studies of electrospun nano-scale composite fibers. *J Therm Anal Calorim.* 2011;107:1237–42.
 16. Noori M, Ravari F, Ehsani M. Preparation of PVA nanofibers reinforced with magnetic graphene by electrospinning method and investigation of their degradation kinetics using master plot analyses on solid state. *J Therm Anal Calorim.* 2018;132:397–406. <https://doi.org/10.1007/s10973-017-6927-7>.
 17. Li Y, Yang H, Hong Y, Yang Y, Cheng Y. Electrospun nanofiber-based nanoboron/nitrocellulose composite and their reactive properties. *J Therm Anal Calorim.* 2017;130:1063–8.
 18. Caratão B, Carneiro E, Sá P, Almeida B, Carvalho S. Properties of electrospun TiO₂ nanofibers. *J Nanotechnol. Hindawi;* 2014 [cited 2018 May 23];2014:1–5. <http://www.hindawi.com/journals/jnt/2014/472132/>.
 19. Su Y, Wang B, Liu L, Wang G, Qi H, Li Z, et al. Electrospinning of a porous silica fiber-confined titanium dioxide catalyst for the degradation of methyl orange. *J Nanoparticle Res.* 2018;20:280. <https://doi.org/10.1007/s11051-018-4377-1>.
 20. Barakat NAM, Abadir MF, Sheikh FA, Kanjwal MA, Park SJ, Kim HY. Polymeric nanofibers containing solid nanoparticles prepared by electrospinning and their applications. *Chem Eng J.* 2010;156:487–95.
 21. Castellano M, Alloisio M, Darawish R, Dodero A, Vicini S. Electrospun composite mats of alginate with embedded silver nanoparticles. *J Therm Anal Calorim.* 2019;0123456789. <https://doi.org/10.1007/s10973-018-7979-z>.
 22. Szilágyi IM, Santala E, Heikkilä M, Pore V, Kemell M, Nikitin T, et al. Photocatalytic properties of WO₃/TiO₂ core/shell nanofibers prepared by electrospinning and atomic layer deposition. *Chem Vap Depos.* 2013;19:149–55.
 23. Watthanaarun J, Pavarajarn V, Supaphol P. Science and technology of advanced materials. 2005 [cited 2018 May 23]; <http://iopscience.iop.org/article/10.1016/j.stam.2005.02.002/pdf>.
 24. Jia L, Qin XH. The effect of different surfactants on the electrospinning poly (vinyl alcohol)(PVA) nanofibers. *J Therm Anal Calorim.* 2013;112:595–605.
 25. Katsumata KI, Ohno Y, Tomita K, Sakai M, Nakajima A, Kakihana M, et al. Preparation of TiO₂ thin films using water-soluble titanium complexes and their photoinduced properties. *Photochem Photobiol.* 2011;87:988–94.
 26. Zhang Z, Brown S, Goodall JBM, Weng X, Thompson K, Gong K, et al. Direct continuous hydrothermal synthesis of high surface area nanosized titania. *J Alloys Compd.* 2009;476:451–6.
 27. Kim J-H, Fujita S, Shiratori S. Fabrication and characterization of TiO₂ thin film prepared by a layer-by-layer self-assembly method. *Thin Solid Films.* 2006;499:83–9.
 28. Möckel H, Giersig M, Willig F. Formation of uniform size anatase nanocrystals from bis(ammonium lactato)titanium dihydroxide by thermohydrolysis. *J Mater Chem.* 1999;9:3051–6.
 29. Mayya KS, Gittins DI, Caruso F. Gold-titania core-shell nanoparticles by polyelectrolyte complexation with a titania precursor the nanoscale coating of colloid particles with materials of different composition is currently an active area proaches widely used for the surface modifi. *Chem Mater.* 2001;13:3833–6.
 30. Lee S, Sigmund WM. Formation of anatase TiO₂ nanoparticles on carbon nanotubes. *Chem Commun.* 2003;9(6):780–1.
 31. Hao Y, Rui Y, Li Y, Zhang Q, Wang H. Size-tunable TiO₂ nanocrystals from titanium (IV) bis (ammonium lactato) dihydroxide and towards enhance the performance of dye-sensitized solar cells. *Electrochim Acta.* 2014;117:268–75.
 32. Nakane K, Yasuda K, Ogihara T, Ogata N, Yamaguchi S. Formation of poly(vinyl alcohol)-titanium lactate hybrid nanofibers and properties of TiO₂ nanofibers obtained by calcination of the hybrids. *J Appl Polym Sci.* 2007;104:1232–5. <https://doi.org/10.1002/app.25769>.
 33. Song C, Dong X. Preparation and characterization of tricomponent SiO₂/SnO₂/TiO₂ composite nanofibers by electrospinning. *Optoelectron Adv Mater.* 2012;6:225–9.
 34. Santala E, Heikkilä M, Miklo I, Kemell M, Nikitin T, Khriachtchev L, et al. Thermal study on electrospun polyvinylpyrrolidone/ammonium metatungstate nanofibers: optimizing the annealing conditions for obtaining WO₃ nanofibers. *J Therm Anal Calorim.* 2011;105:73–81.
 35. Mishra S, Ahrenkiel SP. Synthesis and Characterization of electrospun nanocomposite TiO₂ nanofibers with Ag nanoparticles for photocatalysis applications. *J Nanomater.* 2012:902491.
 36. Cieślak M, Puchowicz D, Kamińska I. SEM / EDS and Raman micro-spectroscopy examination of titanium-modified polypropylene fibres. *FIBRES Text East Eur.* 2014;3:47–53.
 37. Kiennork S, Nakhwong R, Chueachot R. Preparation and characterization of electrospun TiO₂ nanofibers via electrospinning preparation and characterization of electrospun. *Integr Ferroelectr.* 2015;4587.
 38. Sivaiah K, Kumar KN, Naresh V, Buddhudu S. Structural and optical properties of Li⁺: PVP & Ag⁺: PVP polymer films. *Mater Sci Appl.* 2011;2011:1688–96.
 39. Thamaphat K, Limsuwan P, Ngotawornchai B. Phase characterization of TiO₂ powder by XRD and TEM [Internet]. *Nat. Sci.* 2008. <http://www.thaiscience.info/journals/Article/TKJN/10506878.pdf>.

Publisher's Note Springer Nature remains neutral with regard to jurisdictional claims in published maps and institutional affiliations.